

# Results from the STAR Beam Energy Scan Program

Lokesh Kumar (for the STAR Collaboration)

*Department of Physics, Kent State University, USA*

---

## Abstract

The main aim of the beam energy scan (BES) program at the Relativistic Heavy-Ion Collider (RHIC) is to explore the quantum chromodynamics (QCD) phase diagram. The specific physics goal is to search for the phase boundary and the QCD critical point. We present results from Au+Au collisions at various energies collected in the BES program by the Solenoidal Tracker At RHIC (STAR) experiment. First results on transverse momentum ( $p_T$ ) spectra,  $dN/dy$ , and average transverse mass ( $\langle m_T \rangle$ ) for identified hadrons produced at mid-rapidity for  $\sqrt{s_{NN}} = 7.7$  GeV are presented. Centrality dependence of  $dN/dy$  and  $\langle p_T \rangle$  are also discussed and compared to corresponding data from other energies. In addition, first results on charged hadron directed ( $v_1$ ) and elliptic flow ( $v_2$ ) for  $\sqrt{s_{NN}} = 7.7, 11.5, \text{ and } 39$  GeV are presented. New results on event-by-event fluctuations (particle ratio, net-proton and net-charge higher moments) are presented for  $\sqrt{s_{NN}} = 39$  GeV.

---

## 1. Introduction

The Relativistic Heavy-Ion Collider at Brookhaven National Laboratory (BNL) is built to study the properties of a new state of matter, called Quark Gluon Plasma (QGP). One of the major goals of heavy-ion collision experiments is to explore the QCD phase diagram. The QCD phase diagram consists mainly two phases - the QGP phase, where the relevant degrees of freedom are quarks and gluons, and the hadronic phase. Finite temperature lattice QCD calculations [1] at baryon chemical potential  $\mu_B = 0$  suggest a cross-over above a critical temperature  $T_c \sim 170 - 190$  MeV from the hadronic to the QGP phase. At large  $\mu_B$ , several QCD based calculations [2] predict the quark-hadron phase transition to be of the first order. The point in the QCD phase plane ( $T$  vs.  $\mu_B$ ) where the first order phase transition ends is the QCD critical point. The BES program at RHIC [3,4] aims to search the QCD phase boundary and QCD critical point. The QCD phase diagram can be accessed by varying temperature  $T$  and baryonic chemical potential  $\mu_B$ . Experimentally this can be achieved by varying the colliding beam energy. The STAR took data in the year 2010 for the beam energies  $\sqrt{s_{NN}} = 7.7$  GeV, 11.5 GeV, and 39 GeV as a first phase of the BES program.

Table 1

The BES energies, corresponding  $\mu_B$  values [9], and total events with a minimum bias (MB) trigger collected by STAR during the BES run in 2010.

$\sqrt{s_{NN}}$ (GeV)	$\mu_B$ (MeV)	Events (Million MB)
7.7	410	5
11.5	300	7.5
39	112	250

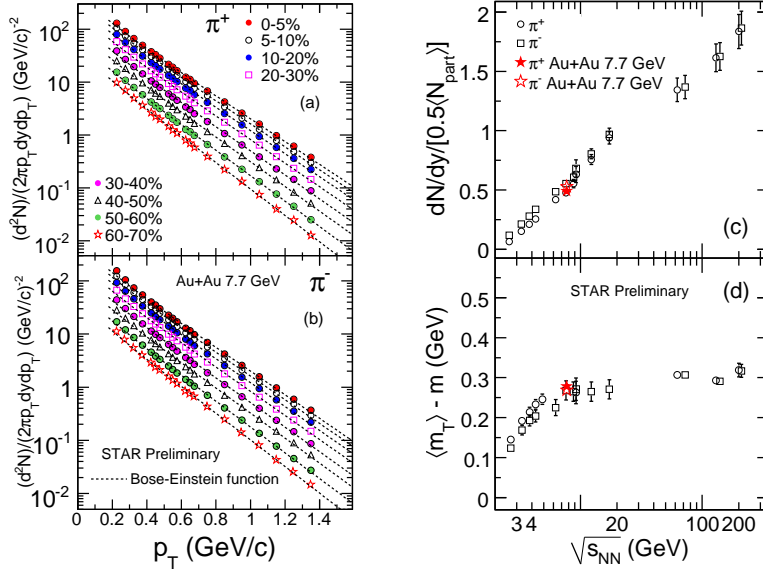


Fig. 1. (color online) Left panel: Transverse momentum spectra for charged pions at mid-rapidity ( $|y| < 0.1$ ) in Au+Au collisions at  $\sqrt{s_{NN}} = 7.7$  GeV. The lines are the Bose-Einstein fits to the distributions. Right panel: (c)  $dN/dy$  normalized by  $\langle N_{\text{part}} \rangle / 2$  and (d)  $\langle m_T \rangle - m$  of  $\pi^\pm$ , plotted as a function of collision energy. See text for details. The errors shown are the quadratic sum of statistical and systematic uncertainties, except for  $\sqrt{s_{NN}} = 7.7$  GeV, which has only statistical errors.

The results presented here are based on data taken at STAR [5] for Au+Au collisions at  $\sqrt{s_{NN}} = 7.7, 11.5,$  and  $39$  GeV in the year 2010. The main detector subsystem used for particle identification is the Time Projection Chamber (TPC) [6]. Particle identification is enhanced up to higher  $p_T$  with the recent inclusion of full barrel Time Of Flight (TOF) [7] detector. The raw yields are extracted at low- $p_T$  using ionization energy loss ( $dE/dx$ ) from TPC, and at higher  $p_T$  using TOF information. The identified particle results are presented for the mid-rapidity  $|y| < 0.1$  region. Directed flow results are obtained using the Beam Beam Counter (BBC) which provides event plane determination at forward pseudorapidities ( $3.8 \leq |\eta| \leq 5.2$ ). Event planes used for the elliptic flow results are provided by both TPC ( $|\eta| < 1$ ) and Forward Time Projection Chamber (FTPC) [8] ( $2.5 \leq |\eta| \leq 4.2$ ). Table 1 lists the BES energies, corresponding  $\mu_B$  values, and total events collected by STAR during the BES program in the year 2010.

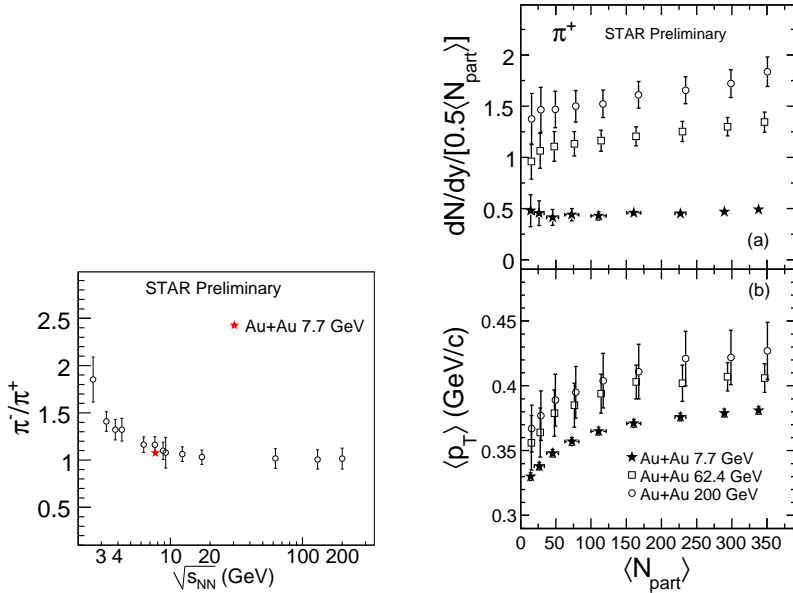


Fig. 2. Left panel (color online):  $\pi^-/\pi^+$  ratio at mid-rapidity ( $|y| < 0.1$ ) for central 0–5% Au+Au collisions at  $\sqrt{s_{NN}} = 7.7$  GeV compared to previous results from AGS [10], SPS [11], and RHIC [3,12]. Right Panel: (a)  $dN/dy$  normalized by  $\langle N_{\text{part}} \rangle / 2$  and (b)  $\langle p_T \rangle$  of  $\pi^+$ , plotted as a function of  $\langle N_{\text{part}} \rangle$ . The errors shown are quadratic sum of statistical and systematic uncertainties, except for  $\sqrt{s_{NN}} = 7.7$  GeV, which has only statistical errors.

## 2. Results

### 2.1. Transverse momentum spectra at $\sqrt{s_{NN}} = 7.7$ GeV

Figure 1 (left panel) shows the transverse momentum spectra for  $\pi^\pm$  in Au+Au collisions at  $\sqrt{s_{NN}} = 7.7$  GeV. The results are shown for various collision centrality classes as listed in the figure. The pion spectra presented here have been corrected for the weak decay feed-down and muon contamination. The particle production can be characterized by studying the  $dN/dy$  and  $\langle m_T \rangle - m$  for the produced hadrons, where  $m$  is the mass of the hadron and  $m_T = \sqrt{m^2 + p_T^2}$  is its transverse mass. These are discussed in the next section.

### 2.2. Energy dependence of yield, $\langle m_T \rangle$ , and anti-particle to particle ratio

Figure 1 (c) shows  $dN/dy$  normalized by  $\langle N_{\text{part}} \rangle / 2$  for  $\pi^\pm$  in 0–5% central Au+Au collisions at  $\sqrt{s_{NN}} = 7.7$  GeV and are compared to previous results at AGS [10], SPS [11], and RHIC [3,12]. Within errors, the yields are consistent with previous results at similar  $\sqrt{s_{NN}}$ . The  $\pi^-/\pi^+$  ratio at  $\sqrt{s_{NN}} = 7.7$  GeV is around 1.1 (Fig. 2 left panel). Figure 1 (d) shows the  $\langle m_T \rangle - m$  for  $\pi^\pm$  in 0–5% central Au+Au collisions at  $\sqrt{s_{NN}} = 7.7$  GeV.

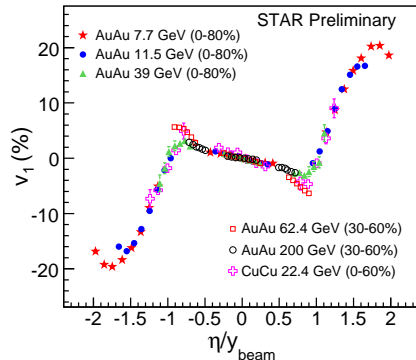


Fig. 3. (color online) Charged hadron  $v_1$  vs.  $\eta/y_{\text{beam}}$ . The errors shown are statistical.

The results are also compared to previous measurements at AGS [10], SPS [11], and RHIC [3,12]. The results from Au+Au collisions at  $\sqrt{s_{NN}} = 7.7$  GeV are consistent with corresponding measurements at SPS energies at similar  $\sqrt{s_{NN}}$ . Both  $dN/dy$  and  $\langle m_T \rangle - m$  are obtained using data in the measured  $p_T$  ranges and extrapolating using a Bose-Einstein functional form for the unmeasured  $p_T$  ranges. For the present mid-rapidity measurements, the contribution to the yields from extrapolation to the total yield is about 30% for  $\pi^\pm$ .

The  $\langle m_T \rangle - m$  values increase with  $\sqrt{s_{NN}}$  at lower AGS energies, stay independent of  $\sqrt{s_{NN}}$  at the SPS and RHIC 7.7 GeV collisions, then tend to somewhat rise further with increasing  $\sqrt{s_{NN}}$  at the higher beam energies at RHIC. For a thermodynamic system,  $\langle m_T \rangle - m$  can be an approximate representation of the temperature of the system, and  $dN/dy \propto \ln(\sqrt{s_{NN}})$  may represent the entropy. In such a scenario, these observations could reflect the characteristic signature of a first order phase transition, as proposed by Van Hove [13]. However, there could be several other effects to which  $\langle m_T \rangle - m$  is sensitive, which also need to be understood for proper interpretation of the data [14].

### 2.3. Centrality dependence of $dN/dy$ and $\langle p_T \rangle$

Figure 2 (right panel) shows (a) the comparison of collision centrality dependence of  $dN/dy$  of  $\pi^+$  normalized by  $\langle N_{\text{part}} \rangle / 2$ , between new results at  $\sqrt{s_{NN}} = 7.7$  GeV and previously published results at  $\sqrt{s_{NN}} = 62.4$  and 200 GeV from the STAR experiment [12]. The yields of charged pions decrease with decreasing collision energy. At low energy,  $dN/dy/[0.5\langle N_{\text{part}} \rangle]$  for charged pions is almost constant as a function of collision centrality. This supports the idea that particle production is dominated by soft processes at 7.7 GeV. Right panel (b) of Fig. 2 shows the comparison of  $\langle p_T \rangle$  as a function of  $\langle N_{\text{part}} \rangle$  for  $\pi^+$  from Au+Au collisions at  $\sqrt{s_{NN}} = 7.7$  GeV with the same from collisions at  $\sqrt{s_{NN}} = 62.4$  and 200 GeV [12]. For the collision centralities studied, the dependencies of  $\langle p_T \rangle$  on  $\langle N_{\text{part}} \rangle$  at  $\sqrt{s_{NN}} = 7.7$  GeV are similar to those at  $\sqrt{s_{NN}} = 62.4$  and 200 GeV. The values of  $\langle p_T \rangle$  increase from peripheral to central collisions. This indicates that collectivity increases with collision centrality. The  $\langle p_T \rangle$  values also increase with collision energy.

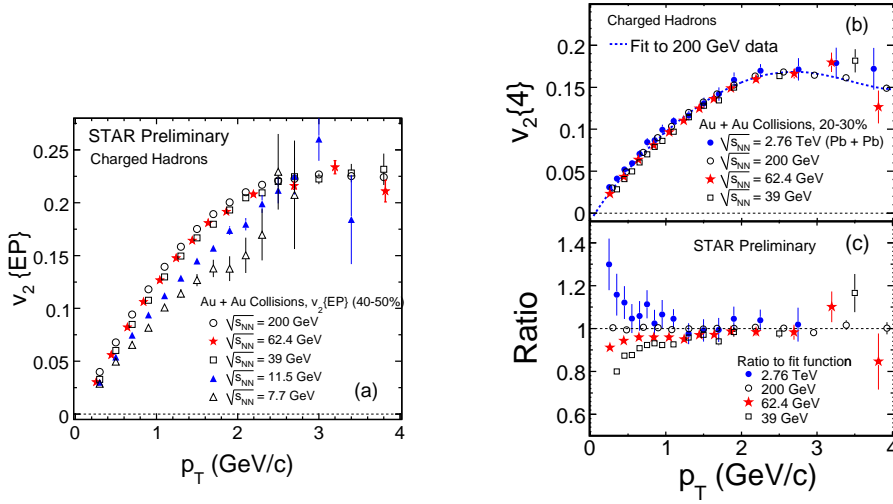


Fig. 4. (color online) Left panel: (a)  $v_2$  obtained from event plane method plotted as a function of  $p_T$  for charged hadrons. The error bars include only statistical uncertainties. Right panel: (b)  $v_2$  obtained using the 4-particle cumulant method plotted as a function of  $p_T$  for charged hadrons. The line represents the fit to 200 GeV data. (c) Ratio of the fit in (b) to  $v_2$  from all the energies as a function of  $p_T$ .

#### 2.4. Azimuthal anisotropy

There are two types of azimuthal anisotropy that are widely studied in heavy-ion collisions, directed flow  $v_1$  and elliptic flow  $v_2$ . Directed flow measurements at forward rapidities describe the “side-splash” motion of the collision products. The dependence of  $v_1$  on  $\eta$  around mid-rapidity is discussed in the literature as a possible signature of a first order phase transition [15]. Elliptic flow provides the possibility to gain information about the degree of thermalization of the hot, dense medium.

Figure 3 shows charged hadron  $v_1$  results for the 0–80% Au+Au collisions at  $\sqrt{s_{NN}} = 7.7$  GeV, 11.5 GeV, and 39 GeV. These are compared to corresponding results from 30–60% Au+Au collisions at  $\sqrt{s_{NN}} = 62.4$ , 200 GeV [16], and 0–60% Cu+Cu collisions at  $\sqrt{s_{NN}} = 22.4$  GeV [17]. The mid-rapidity region corresponds to the produced particles, while the forward rapidity corresponds to the transported particles. At mid-rapidity, all the results have comparable values. At forward rapidity, the trend of  $v_1$  is energy dependent [3]. When  $|\eta|$  is scaled with the corresponding beam rapidities ( $y_{\text{beam}}$ ) for different energies, a universal curve is obtained as shown in the figure for the measured  $|\eta|/y_{\text{beam}} < 0.5$  range. The  $y_{\text{beam}}$  for  $\sqrt{s_{NN}} = 7.7$ , 11.5, 39, 22.4, 62.4, and 200 GeV are 2.1, 2.5, 3.2, 3.7, 4.2, and 5.4 respectively.

Figure 4 (a) shows  $v_2$  obtained from event plane method [18] plotted as a function of  $p_T$  for charged hadrons in 40–50% Au+Au collisions at  $\sqrt{s_{NN}} = 7.7$ , 11.5, and 39 GeV. The results are compared to corresponding results from  $\sqrt{s_{NN}} = 62.4$  and 200 GeV [19]. The figure shows that  $v_2(p_T)$  at 7.7 GeV is smaller than that at 11.5 GeV which is smaller than that at 39 GeV, suggesting that elliptic flow increases as the BES energies increase. Right panel (b) shows  $v_2$  obtained using the 4-particle cumulant method [20]

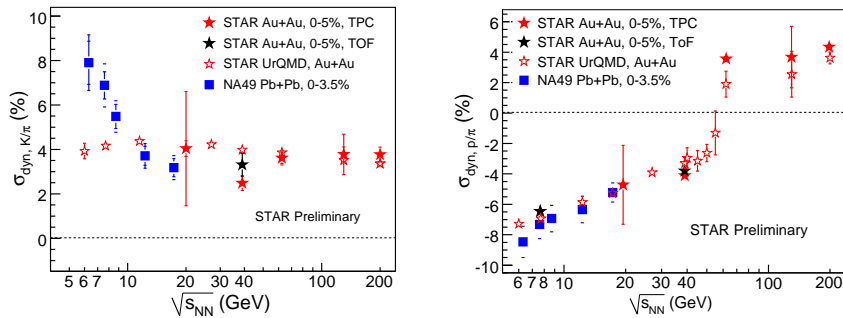


Fig. 5. (color online) Left panel:  $K/\pi$  fluctuations expressed as  $\sigma_{\text{dyn}}$ , plotted as a function of collision energy. The errors are quadratic sum of systematic and statistical uncertainties except for  $\sqrt{s_{NN}} = 39$  GeV, which has only statistical errors. Right panel: same as (a) but for  $p/\pi$  fluctuations.

plotted as a function of  $p_T$  for charged hadrons in 20–30% Au+Au collisions at  $\sqrt{s_{NN}} = 39, 62.4,$  and 200 GeV, from STAR. The results are compared with corresponding results in Pb+Pb collisions at  $\sqrt{s_{NN}} = 2.76$  TeV, from the ALICE experiment [21]. The line represents the fifth-order polynomial fit to 200 GeV data. Panel (c) shows the ratio of the fit to  $v_2$  from all the energies as a function of  $p_T$ . It is observed that  $v_2\{4\}(p_T)$  for all the energies show similar values (within  $\sim 10\%$  from 200 GeV data) beyond  $p_T = 500$  MeV/ $c$ . This saturation is very interesting considering the wide energy range 39 GeV to 2.76 TeV.

## 2.5. Fluctuations

The non-monotonic behavior of fluctuations in the particle ratios such as  $K/\pi$  and  $p/\pi$  as a function of collision energy could indicate the presence of a QCD critical point or the phase transition. These ratio fluctuations are quantified by the variable  $\nu_{\text{dyn}}$  [22]. Earlier measurements [23] of particle ratio fluctuations used the variable given by:  $\sigma_{\text{dyn}} = \text{sign}(\sigma_{\text{data}}^2 - \sigma_{\text{mixed}}^2) \sqrt{|\sigma_{\text{data}}^2 - \sigma_{\text{mixed}}^2|}$ , where  $\sigma$  is the relative width of the  $K/\pi$  and  $p/\pi$  distribution in either real data or mixed events. It has been shown that  $\sigma_{\text{dyn}}^2 \approx \nu_{\text{dyn}}$ .

Figure 5 (left panel) shows the energy dependence of dynamical  $K/\pi$  fluctuations expressed as  $\sigma_{\text{dyn}}$  [24]. The 0-3.5% central Pb+Pb collisions NA49 results (solid squares) show decrease in dynamical fluctuations as a function of collision energy. The 0-5% central Au+Au collisions STAR results (solid stars) for  $\sqrt{s_{NN}} = 19.6, 62.4, 130$  and 200 GeV, are constant as a function of beam energy. The newly measured  $K/\pi$  fluctuation results from 0-5% central Au+Au collisions at  $\sqrt{s_{NN}} = 39$  GeV are similar to other STAR results [22]. The UrQMD model calculations (open stars) using the STAR detector acceptance, give approximately 4%  $K/\pi$  fluctuations for all the beam energies. The right panel of Fig. 5 shows the energy dependence of dynamical  $p/\pi$  fluctuations expressed as  $\sigma_{\text{dyn}}$  [24]. The STAR results (solid stars) from 0-5% central Au+Au collisions are compared with those from 0-3.5% central Pb+Pb collisions from the NA49 experiment (solid squares). The new results from 0-5% central Au+Au collisions at  $\sqrt{s_{NN}} = 7.7$  and 39 GeV are also shown. All the data points show increase in  $p/\pi$  fluctuations as a function of beam energy. The STAR results from 7.7 GeV are in close agreement with those from the NA49 experiment

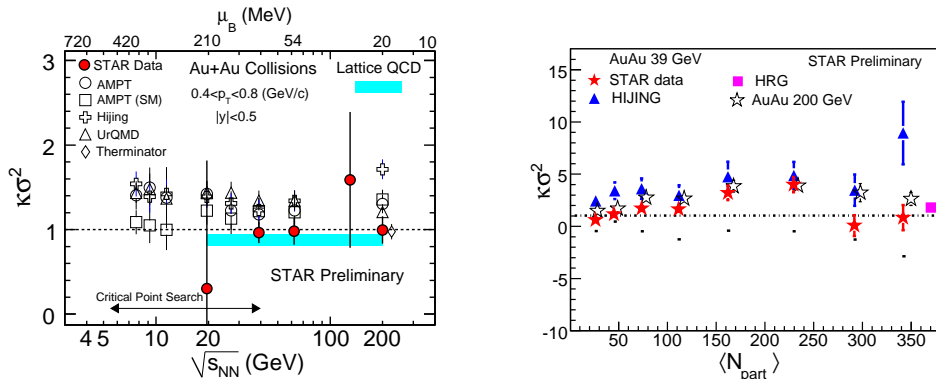


Fig. 6. (color online) Left panel:  $\sqrt{s_{NN}}$  dependence of  $\kappa\sigma^2$  for net-proton distributions measured at RHIC. Errors are quadratic sum of systematic and statistical uncertainties, except for  $\sqrt{s_{NN}} = 39$  GeV, which has only statistical errors. Right panel:  $\kappa\sigma^2$  for net-charge distributions as a function of  $\langle N_{part} \rangle$ . Results from  $\sqrt{s_{NN}} = 39$  GeV are compared with those from  $\sqrt{s_{NN}} = 200$  GeV [27]. Also shown are the calculations from the HIJING and HRG models.

at similar  $\sqrt{s_{NN}}$ . The UrQMD model calculations (open stars) after correcting for the STAR detector acceptance reproduce the increasing trend seen in data as a function of beam energy. The STAR results presented here are from the similar  $p_T$  ranges (pion, kaon: 0.2–0.6 GeV/ $c$  and proton: 0.4–1.0 GeV/ $c$ ) for both TPC and TOF.

It has been shown that higher moments of distributions of conserved quantities (net-baryon number, net-strangeness and net-charge), measuring deviations from a Gaussian, are sensitive to the critical point fluctuations [25]. The moments, standard deviation  $\sigma$ , skewness  $S$ , and kurtosis  $\kappa$ , of conserved quantities distributions, are defined as:  $\sigma = \sqrt{\langle (N - \langle N \rangle)^2 \rangle}$ ,  $S = \langle (N - \langle N \rangle)^3 \rangle / \sigma^3$ , and  $\kappa = \langle (N - \langle N \rangle)^4 \rangle / \sigma^4 - 3$ , respectively. The products of the moments such as  $\kappa\sigma^2$  and  $S\sigma$ , are related to the ratio of conserved quantities number susceptibilities ( $\chi$ ) at a given temperature ( $T$ ) computed in QCD models as:  $S\sigma \sim \chi^{(3)} / \chi^{(2)}$  and  $\kappa\sigma^2 \sim \chi^{(4)} / \chi^{(2)}$ . Close to a critical point, models predict the conserved quantities number distributions to be non-Gaussian and susceptibilities to diverge causing  $S\sigma$  and  $\kappa\sigma^2$  to deviate from constants and have large values.

Figure 6 (left panel) shows the energy dependence of  $\kappa\sigma^2$  for net-proton distributions, compared to several model calculations that do not include a critical point. The  $\kappa\sigma^2$  as a function of the beam energy does not show any non-monotonic behavior and is consistent with unity. The new STAR result for  $\kappa\sigma^2$  from  $\sqrt{s_{NN}} = 39$  GeV is consistent with previous STAR measurements [26]. The right panel shows the  $\kappa\sigma^2$  for net-charge distributions as a function of  $\langle N_{part} \rangle$ . STAR results for  $\sqrt{s_{NN}} = 39$  and 200 GeV are consistent with each other. HIJING results are consistent with the data except for the most central collisions. The  $\kappa\sigma^2$  for central collisions is consistent with the hadron resonance gas (HRG) model [28] which assumes thermal equilibrium.

### 3. Summary

The RHIC beam energy scan program has started. The aim of the BES program is to search for the QCD phase boundary and QCD critical point. In the first phase of the BES

program, the STAR experiment took data for the beam energies  $\sqrt{s_{NN}} = 7.7, 11.5,$  and  $39$  GeV during 2010. The event statistics goals for three beam energies were achieved. The first results from the BES program are presented in this paper. Measurements of identified particle production at  $\sqrt{s_{NN}} = 7.7$  GeV suggest that particle production scales with  $\langle N_{\text{part}} \rangle$ . The measurements of  $\langle p_T \rangle$  as a function of collision centrality indicate that the collectivity increases with collision centrality. The mid-rapidity  $\pi^-/\pi^+$  ratio at  $\sqrt{s_{NN}} = 7.7$  GeV is close to 1.1. Directed flow results for all the beam energies scale with  $\eta/y_{\text{beam}}$  (for measured  $|\eta|/y_{\text{beam}} < 0.5$  range), extending the already established scaling behavior down to 7.7 GeV. The  $v_2\{4\}(p_T)$  shows saturation above  $p_T = 500$  MeV/c for all the beam energies from 39 GeV through 2.76 TeV. Particle ratio fluctuations for the energies presented are consistent with the established trends. The net-proton and net-charge results are consistent with the HRG model.

We wish to acknowledge the support from DOE.

## References

- [1] Y. Aoki *et al.*, Nature **443**, 675 (2006).
- [2] S. Ejiri, Phys. Rev. D **78**, 074507 (2008); E.S. Bowman *et al.*, Phys. Rev. C **79**, 015202 (2009).
- [3] B. I. Abelev *et al.* (STAR Collaboration), Phys. Rev. C **81**, 024911 (2010); STAR Internal Note - SN0493, 2009; L. Kumar (STAR Collaboration), Nucl. Phys. A **830**, 275C (2009).
- [4] B. Mohanty, Nucl. Phys. A **830**, 899C (2009).
- [5] K. H. Ackermann *et al.*, Nucl. Instrum. Methods A **499**, 624 (2003).
- [6] M. Anderson *et al.*, Nucl. Instrum. Methods A **499**, 659 (2003).
- [7] W. J. Llope *et al.*, Nucl. Instrum. Methods B **241**, 306 (2005).
- [8] K. H. Ackermann *et al.*, Nucl. Instrum. Methods A **499**, 713 (2003).
- [9] J. Cleymans *et al.*, Phys. Rev. C **73**, 034905 (2006).
- [10] L. Ahle *et al.* (E866 Collaboration and E917 Collaboration), Phys. Lett. B **490**, 53 (2000); L. Ahle *et al.* (E866 Collaboration and E917 Collaboration), *ibid.* B **476**, 1 (2000); J. L. Klay *et al.* (E895 Collaboration), Phys. Rev. Lett. **88**, 102301 (2002).
- [11] S. V. Afanasiev *et al.* (NA49 Collaboration), Phys. Rev. C **66**, 054902 (2002); C. Alt *et al.* (NA49 Collaboration), *ibid.* **77**, 024903 (2008); **73**, 044910 (2006); T. Anticic *et al.* (NA49 Collaboration), *ibid.* **69**, 024902 (2004).
- [12] B. I. Abelev *et al.* (STAR Collaboration), Phys. Rev. C **79**, 034909 (2009); J. Adams *et al.* (STAR Collaboration), Phys. Rev. Lett. **92**, 112301 (2004).
- [13] L. Van Hove, Phys. Lett. B **118**, 138 (1982).
- [14] B. Mohanty *et al.*, Phys. Rev. C **68**, 021901 (2008) and references therein.
- [15] R. Snellings *et al.*, Phys. Rev. Lett. **84**, 2803 (2000); J. Brachmann *et al.*, Phys. Rev. C **61**, 024909 (2000); L. P. Csernai and D. Rohrlich, Phys. Lett. B **458**, 454 (1999); H. Stoecker, Nucl. Phys. A **750**, 121 (2005).
- [16] B. I. Abelev *et al.* (STAR Collaboration), Phys. Rev. Lett. **101**, 252301 (2008).
- [17] Y. Pandit, talk at RHIC and AGS users meeting, 2010.
- [18] A. M. Poskanzer and S. A. Voloshin, Phys. Rev. C **58**, 1671 (1998).
- [19] B. I. Abelev *et al.* (STAR Collaboration), Phys. Rev. C **77**, 054901 (2008); *ibid.* **75**, 054906.
- [20] N. Borghini, P. M. Dinh, and J.-Y. Ollitrault, Phys. Rev. C **64**, 054901 (2001).
- [21] K. Aamodt *et al.* (ALICE Collaboration), arXiv:1011.3914 [nucl-ex].
- [22] B. I. Abelev *et al.* (STAR Collaboration), Phys. Rev. Lett. **103**, 092301 (2009).
- [23] C. Alt *et al.* (NA49 Collaboration), Phys. Rev. C **79**, 044910 (2009).
- [24] T. Tarnowsky, arXiv:1101.3351 [nucl-ex].
- [25] M. A. Stephanov, Phys. Rev. Lett. **102**, 032301 (2009).
- [26] M. M. Aggarwal *et al.* (STAR Collaboration), Phys. Rev. Lett. **105**, 022301 (2010).
- [27] T. K. Nayak (for the STAR Collaboration), Nucl. Phys. A **830**, 555 (2009).
- [28] F. Karsch and K. Redlich, Phys. Lett. B **695**, 136 (2011).